# Journal Pre-proof

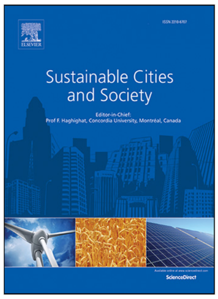


Effects of urbanization and topography on thermal comfort during a heat wave event: A case study of Fuzhou, China

Zefeng Zheng, Xinlu Lin, Li Chen, Chao Yan, Ting Sun

PII: S2210-6707(24)00062-3
DOI: https://doi.org/10.1016/j.scs.2024.105233
Reference: SCS 105233

To appear in: *Sustainable Cities and Society*

Received date : 5 December 2023
Revised date : 21 January 2024
Accepted date : 23 January 2024

Please cite this article as: Z. Zheng, X. Lin, L. Chen et al., Effects of urbanization and topography on thermal comfort during a heat wave event: A case study of Fuzhou, China. *Sustainable Cities and Society* (2024), doi: https://doi.org/10.1016/j.scs.2024.105233.

This is a PDF file of an article that has undergone enhancements after acceptance, such as the addition of a cover page and metadata, and formatting for readability, but it is not yet the definitive version of record. This version will undergo additional copyediting, typesetting and review before it is published in its final form, but we are providing this version to give early visibility of the article. Please note that, during the production process, errors may be discovered which could affect the content, and all legal disclaimers that apply to the journal pertain.

© 2024 Published by Elsevier Ltd.

Journal Pre-proof

# Graphical Abstract [1]

**Effects of urbanization and topography on thermal comfort during a heat wave event: a case study of Fuzhou, China**

Zefeng Zheng, Xinlu Lin, Li Chen, Chao Yan, Ting Sun


[1] First Author and Second Author contributed equally to this work

Journal Pre-proof

Journal Pre-proof

# Effects of urbanization and topography on thermal comfort during a heat wave event: a case study of Fuzhou, China

Zefeng Zheng[a], Xinlu Lin[a,b,1,], Li Chen[c], Chao Yan[b], Ting Sun[d]

[a]*College of Civil Engineering, Fuzhou University, Fuzhou 350108, China*
[b]*Key Laboratory of Urban Meteorology, China Meteorological Administration, Beijing 100089, China*
[c]*Fujian Climate Center, Fuzhou 350007, UK*
[d]*Institute for Risk and Disaster Reduction, University College London, London, UK*

**Abstract**

Urbanization intensifies urban heat and compromises thermal comfort. However, few studies have examined the interactions of Urban Heat Island (UHI) between neighboring cities and the impacts of expanding satellite towns on central urban areas (CUA). We conducted a series of WRF/BEP-BEM simulations during a summer heat wave in Fuzhou, China, to understand how extensive urbanization and complex topography affect thermal comfort. Control runs reveal an intense UHI centered on Fuzhou's CUA. Comparisons with scenarios where urban land use and terrain are altered demonstrate that urbanization degrades thermal comfort citywide by elevating heat stress while valley-basin topography worsens midday heat but alleviates nighttime humidity. The urban heat island circulation above the CUA suppresses the valley wind circulation and prevents the sea breeze front from advancing inland in the afternoon. Notably, CUA urbanization enhances sea breezes in a satellite town, inducing afternoon "cool islands". Interactions between CUA and satellite towns appear minimized, with urbanization impacts confined locally. Future expansion according to the "Fuzhou 2035" Master Plan shows negligible effects on thermal comfort in CUA. Our findings enhance understanding of intra-urban UHI dynamics in complex terrains. The outcomes directly inform urban planning and climate adaptation strategies to promote Fuzhou's livability and resilience.

*Keywords:* thermal comfort, urban heat island (UHI), WRF, heat wave, WBGT.

* Corresponding author
*Email address:* `linxinlu@fzu.edu.cn` (Xinlu Lin)

## 1. Introduction

Today, more than half of the world's population lives in urban areas; and it is projected that more than two thirds of the global population will be living in cities by 2050 (United Nations, 2020). Such rapid urbanization is aggregating anthropogenic emissions and altering land covers, leading to numerous environmental challenges. A remarkable challenge is the exaggerated human thermal comfort due to the interaction between urban heat islands (UHIs) (Howard, 1833; Oke, 1995) – cities are usually warmer than their rural surroundings – and heat waves (i.e., prolonged overheating periods) that may incur extra deaths (e.g. 580 and 206 in Nagpur, India during 2010 and 2014 events (Dutta et al., 2020)). Moreover, the risk of extreme heat to human health is increasing due to climate change (Lüthi et al., 2023). Therefore, it calls for an urgent need to increase our understanding of human thermal comfort, in particular for developing sustainable cities.

Many studies have investigated the effects of urban surface properties on UHI and human thermal comfort (Garuma, 2018; Wang et al., 2021; Li et al., 2019). The increasing building densities suppress the turbulence and exacerbate the heat stress (Li et al., 2020; Mehrotra et al., 2019; Wang et al., 2021). The replacement of natural landscapes with built-up surfaces enhances the heat storage in cities, which contributes to the UHI effect (Huang et al., 2019; Ibrahim et al., 2018; Wang et al., 2022). Meanwhile, the continuing expansion of cities exacerbates the UHI, threatening to reduce thermal comfort for urban residents in the future (Shen et al., 2022; Vinayak et al., 2022).

Besides urban surface properties, topography also influences urban thermal comfort (Fernando, 2010; Ganbat et al., 2014; Wu et al., 2021). For instance, the Beijing-Tianjin-Hebei region, one of the most developed urban agglomerations in China, is influenced by the intertwined effects of sea-land breeze circulations, mountain-valley breeze circulations, and urban heat island circulations. This is due to its geographical location with the Bohai Sea to the east and surrounding mountains to the west: the topographically strengthened sea breeze circulation leads to an asymmetric urban heat island circulations during the daytime, and the mountain breeze circulation can combine with the land breeze to form a large circulation that extends from the coast



Journal Pre-proof

Journal Pre-proof

to the mountains at night (Liu et al., 2009; Miao et al., 2015). In Seoul, South Korea, the UHI circulation generated in the plain urban areas far from the mountains is enhanced by the subsidence heating due to the valley wind circulation, which hinders the sea breeze intrusion (Ryu and Baik, 2013). Conversely, in São Paulo, Brazil, topography promotes the propagation of sea breeze by forcing adiabatic cooling of the marine air going up the coastal escarpment, enhancing the temperature gradient between the southern portion of the plateau and the metropolitan region (Ribeiro et al., 2018). However, the above studies rarely isolate the effect of topography on regional thermal comfort.

In addition to the topographical controls, thermal environments of cities are also impacted by their neighboring counterparts. For example, the increase in the urbanization level of the upstream cities may enhance the UHI effect in the downstream ones under the influence of background winds and local circulations (e.g. Shanghai - Kunshan Kang et al. (2014); and Washington–Baltimore Zhang et al. (2009, 2011)). Development of satellite towns – conventionally defined as smaller cities near metropolis to facilitate regional socioeconomic development – may also alter the local climate of the central urban areas (CUAs). To the best of our knowledge, however, there is little literature focusing on the interaction between them.

This work centers on Fuzhou, the capital of China's Fujian Province situated on the southeast coast, whose unique geographical setting incorporates all the previously mentioned factors influencing the local thermal environment. The CUA of Fuzhou lies along the estuary basin of Fujian's largest river, the Min River, while six satellite towns are separated from it by hills or mountains. To build Fuzhou into a modern international metropolis, the Fuzhou Municipal Government is vigorously promoting the construction of a new town (Binhai New Town) along the southeast coast as part of a grand development plan – the Fuzhou Master Plan 2021-2035 (hereafter referred to as "Fuzhou2035"). Meanwhile, it is noted that Fuzhou has become one of the hottest cities in China due to rapid urbanization over the past four decades (China Meteorological Administration, 2012). As such, concerns about potentially exacerbated thermal comfort induced by the development of Binhai New Town have been escalating since the release of the Fuzhou2035 Plan.



Journal Pre-proof

Journal Pre-proof

Although some recent studies based on remote sensing data have looked into the relationship between the land surface temperature (LST) and land use changes in Fuzhou (Cai et al., 2019; Yang et al., 2021; Yao et al., 2022; You et al., 2021; Yao et al., 2023), how the topography and local atmospheric circulation would influence the local thermal comfort are still yet to be elucidated.

This study aims to investigate the effect of urbanization and topography on the thermal comfort in Fuzhou city during a heat wave event (July 8-14, 2021). Specifically, this work is motivated by the following questions:

(1) How do topography and urbanization, respectively, affect the thermal comfort in Fuzhou?

(2) How do urbanization properties of the CUA and satellite towns affect the thermal comfort of each other? and

(3) Will the development of Binhai New Town increase heat stress in Fuzhou?

To help answer these questions, we adopted the Weather Research and Forecasting (WRF) model, which is a state-of-the-art numerical weather prediction and atmospheric simulation system with proven skill representing land-atmosphere interactions in urban domains (Skamarock et al., 2021; Sanchez et al., 2021; Tan et al., 2023; Zhou et al., 2022).

Through a control simulation evaluated against local observations, we implement WRF coupled with the multi-layer urban canopy model to mimic the Fuzhou's heterogeneous thermal environment during a July 2021 heatwave. A series of sensitivity experiments then systematically quantify the individual and combined effects of realistic topography and land cover change on thermal comfort indicators. Beyond insights to guide Fuzhou's planning and development strategies, this work elucidates physical mechanisms governing urban heat islands in complex coastal terrains - advancing knowledge transferable to other cities pursuing sustainability and resilience.

The remainder of this paper is organized as follows: Section 2 describes the research methodology, experimental design, and model evaluation. Section 3 presents the the results from three aspects: the effects of topography and urbanization; the interplay between the urbanization properties of the CUA and satellite towns; and extreme heat stress. Section 3 also includes a subsec-



Journal Pre-proof

Journal Pre-proof

tion discussing limitations of the modeling approach. Finally, Section 4 summarizes the major conclusions and directions for future research.

## 2. Methods

### *2.1. Study area*

Fuzhou is a mountainous city, in which mountains and hills account for 72.68 % of the total area and the proportion of forest land reaches to 58.36 % (Fig.1). The city center lies at the bottom of the basin, across which the Min River flows into the sea. For several decades, Fuzhou has seen rapid urbanization. Fuzhou's urban population grew from 3.36 million in 2000 to 6.01 million in 2020, with the built-up area expanding from 102 $km^2$ to 305.3 $km^2$ over the same period (Fuzhou Municipal Statistics Bureau, 2021). Six satellite towns – Fuqing (FQ), Changle (CL), Lianjiang (LJ), Minhou (MH), Minqing (MQ), and Yongtai (YT) – have also experienced fast development. According to the "Fuzhou2035", the population of permanent residents will reach 10 million. To satisfy the increasing urban population, the Binhai New Town with an area of 188 $km^2$ is under construction in the Changle area and is expected to be another core built-up area of Fuzhou. Thus, Fuzhou presents an intertwined geographical context shaped by its mountainous terrain, coastal location, ongoing urban expansion, and satellite town development.

### *2.2. Model Configuration*

Numerical simulations were performed with the WRF model version 4.3.1 (Skamarock et al., 2021) with Advanced Research WRF dynamics core developed by the National Center for Atmospheric Research. The WRF model's modular structure easily integrates detailed urban terrain characteristics, such as land use heterogeneity and building morphology, which cannot be resolved in coarse global models. Advanced microphysics and land surface schemes simulate the intricate exchange of energy, momentum, and mass between the urban canopy and the overlying atmosphere. Compared to microscale Computational Fluid Dynamic (CFD) studies limited to small domains or short periods, WRF is capable of mesoscale studies with acceptable computation cost. Compared to resource-intensive microscale computational fluid dynamics studies



Journal Pre-proof

Journal Pre-proof

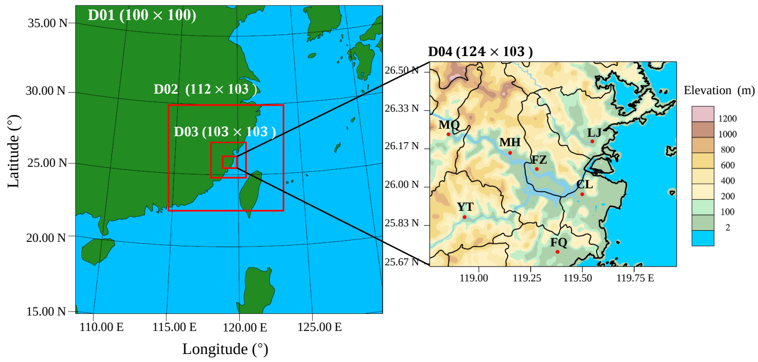


**Fig. 1.** WRF nested domains and terrain in D04 for CTL scenario. Values in parentheses refer to the grids number for nested domains.

limited to small spatial domains or periods, the WRF model strikes an optimal balance of detail and computational efficiency to explore mesoscale processes shaping thermal comfort across metro regions and multi-day heatwaves (Zhang et al., 2011; Ryu and Baik, 2013; Vinayak et al., 2022; Tan et al., 2023).

In WRF model, nested domains allow a need for higher resolution in a specific area, while its background weather conditions can be provided by the larger domains. In our simulations, four one-way (i.e. information exchange is only from the coarse grid to the fine grid) nested domains were used with the horizontal resolutions (grid numbers) of 27 km (100×100), 9 km (112×103), 3 km (103×103) and 1 km (124×103) (Fig.1). The vertical grid has 45 sigma levels (8 levels in the lowest 1km; model top at 50hPa). The NCEP FNL (Final) Operational Global Analysis data were adopted for the initial field and boundary conditions on 1°×1° spatial resolution and 6 h time resolution (National Centers for Environmental Prediction, National Weather Service, NOAA, U.S. Department of Commerce, 2000). The simulations began at 0000 UTC on 7 July and finished at 0000 UTC on 15 July, with the first 24 hours as spin-up time. In the model, some small-scale or too complex atmospheric processes (e.g. cloud and precipitation processes, turbulence of the atmospheric boundary layer, and interactions between the atmosphere and the land surface) are mathematically represented by physical parameterization schemes. The

Journal Pre-proof

physical parameterization schemes we used included the Thompson scheme (Thompson et al., 2004) for the microphysics process, the Grell 3D ensemble cumulus scheme (Grell and Dévényi, 2002) (for Domain 01 and Domain 02 only), the rapid radiative transfer model longwave radiation scheme (RRTM) (Mlawer et al., 1997), the Dudhia shortwave scheme (Dudhia, 1989), the YSU PBL scheme (Hong et al., 2006), the revised MM5 Monin-Obukhov scheme (Zhang and Anthes, 1982), and the Noah-MP land-surface model, which augmented the representations of land surface processes in Noah by implementing multiple parameterization schemes (Niu et al., 2011; Yang et al., 2011). To mimic the effect of urbanization, the multi-layer urban canopy model (MLUCM) incorporating the Building Effects Parameterization (BEP) and the Building Energy Model (BEM) was used. The fluxes from urban impervious surfaces were provided by BEP (Martilli et al., 2002) and the anthropogenic heat of the building was calculated based on the building energy balance by BEM (Salamanca et al., 2010).

Land use and land cover (LULC) data are crucial for accurately predicting urban effects. In recent years, the concept of local climate zone (LCZ) introduced by Oke and Stewart (2012) has been widely used in urban climate research (Brousse et al., 2016; Choudhury et al., 2021; Molnár et al., 2019; Pellegatti Franco et al., 2019). The LCZ scheme includes 10 *urban* and 7 *natural* land cover types; thus, it can well represent the heterogeneity of the urban landscape. In our simulations, the LCZ map of the Fuzhou region was generated following the World Urban Data Access Portal Tool (WUDAPT) level 0 method (Demuzere et al., 2021). The LCZ map data was imported to WRF using the W2W tool (Demuzere et al., 2022). The newly incorporated WUDAPT-LCZ module in WRF version 4.3.1 enabled defining morphological parameters of buildings for each local climate zone type. However, urban grid vegetation information did not get updated through the module integration. To address this limitation and reflect actual urban vegetation, leaf area index (LAI) data was substituted with the GLASS LAI_avhrr (Global LAnd Surface Satellite, Leaf Area Index, Advanced Very High Resolution Radiometer) 0.05° high-precision product (Xiao et al., 2016).



Journal Pre-proof

Journal Pre-proof

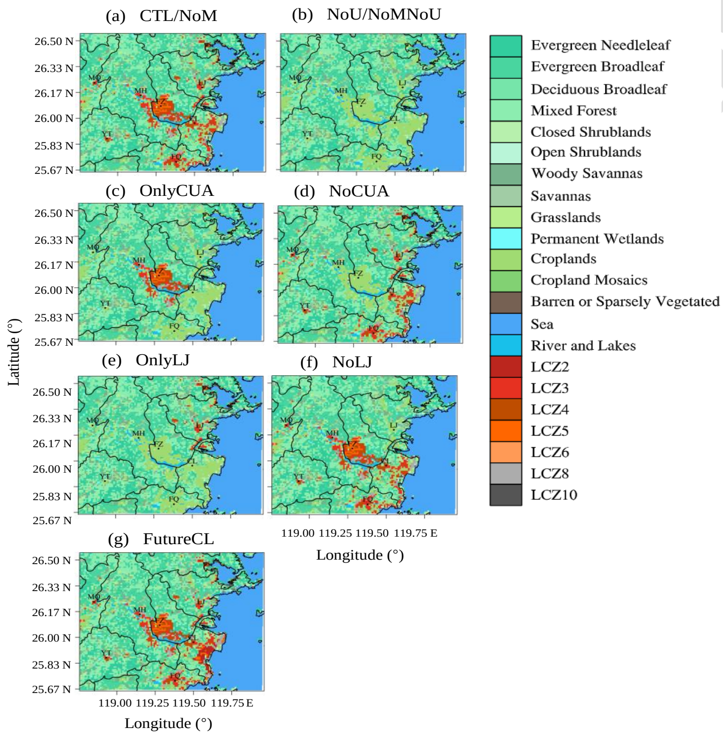


**Fig. 2.** LULC of the simulations (the black nodes denote the locations of the observation stations)

### 2.3. *Experiment Design*

A series of numerical experiments were designed to investigate the impacts of topography and urbanization on the thermal comfort (Table 1, Fig. 2). A control (CTL) experiment was carried out using the current, realistic land use map. Three sensitivity tests separately evaluated topography and urbanization effects:

- NoM: Removed all topography variation by setting grid elevations to zero.

Journal Pre-proof

- NoU: Replaced urban areas with cropland using averaged LAI and GREENFRAC values.
- NoMNoU: Combined NoU cropland replacement with NoM zeroed elevations.

Additionally, the center urban area and a satellite town were studied. NoCUA and NoLJ scenarios were designed according to the CTL test, while the *built* type grid cells in CUA and Lianjiang areas were replaced by the cropland type, respectively. To study the impact of the satellite towns by themselves, the land use maps in CUA and Lianjiang areas under the NoU experiment were replaced with the urban types corresponding to CTL, hereafter referred to as OnlyCUA and OnlyLJ. Furthermore, a simulation named FutureCL was carried out to represent the future urban expansion in the Changle area (i.e. the building of Binhai New Town), in which the land use types were set according to "Fuzhou2035". Specifically, the urban types of Binhai New Town were classified into three types: compact mid-rise (LCZ 2), open mid-rise (LCZ 5), and large low-rise (LCZ 8), which was based on the *GB 50137-2011: Code for classification of urban land use and planning standards of development land* (Ministry of Housing and Urban-Rural Development, PRC, 2011).

Table 1: Design of the Experiments

| Experiment | LCZ parameters | Topography | BEM scheme | Purpose |
|---|---|---|---|---|
| CTL | Yes | Yes | Yes | Real case |
| NoU | No | Yes | No | Influence of Topography and Urbanization |
| NoM | Yes | No | Yes | |
| NoMNoU | No | No | No | |
| NoCUA | Yes (without CUA area) | Yes | Yes | Interactions between CUA and a satellite town |
| OnlyCUA | Yes (only CUA area) | Yes | Yes | |
| NoLJ | Yes (without LJ area) | Yes | Yes | |
| OnlyLJ | Yes (only LJ area) | Yes | Yes | |
| FutureCL | Yes (with Binhai New Town) | Yes | Yes | Influence of development of Binhai New Town |

### *2.4. Model Evaluation*

The observation data obtained from the China Meteorological Data Service Center (`http://data.cma.cn/`) are used to verify the reliability of the WRF model. There are seven stations

Journal Pre-proof

in the innermost simulation domain, which can represent the CUA (Fuzhou station) and six satellite towns (Fig. 1). The model performance is evaluated using mean absolute error (MAE), correlation coefficient (R) and hit rate (HR) between the measurements and the CTL simulation.

$$MAE = \frac{\sum_{i=1}^{N} |F_i - O_i|}{N} \tag{1}$$

$$R = \frac{\frac{1}{N}\sum_{i=1}^{N}\left(F_i - \overline{F}\right)\left(O_i - \overline{O}\right)}{\sqrt{\frac{1}{N}\sum_{i=1}^{N}\left(F_i - \overline{F}\right)^2}\sqrt{\frac{1}{N}\sum_{i=1}^{N}\left(O_i - \overline{O}\right)^2}} \tag{2}$$

$$HR = \frac{num\left(|F_i - O_i| < C\right)}{N} \tag{3}$$

where, $F_i$ represents the modeled simulation value, $\overline{F}$ represents the average of the modeled values, $O_i$ represents the observed value at a specific station, and $\overline{O}$ represents the average of the observed values. $N$ represents the total number of samples, and $C$ represents the threshold. The data used in this study is collected from 7 observation stations, with a total of 169-time steps. Therefore, the number of samples per station is 169, and the total number of samples is 1183. $HR$ represents the ratio of the number of cases where the absolute error between the observed and simulated values is less than the threshold to the total number of samples. In this study, the threshold is set to 2 °C for temperature, 2 m/s for wind speed, and 10% for relative humidity.

The mean absolute error is used as a metric to measure the discrepancy between the model and the actual values. A smaller error indicates a better model performance. The correlation coefficient $R$ is a dimensionless value ranging between -1 and 1. A value of $R$ closer to 1 indicates a closer similarity in the variation trends between the simulated and observed values, suggesting better simulation performance.

### *2.5. Thermal comfort assessment*

Thermal comfort indicates satisfaction with the thermal environment (Epstein and Moran, 2006). It is affected not only by the ambient air temperature but also by humidity, wind speed and even personal factors. In this work, we use Wet Bulb Globe Temperature (WBGT) as a



Journal Pre-proof

Journal Pre-proof

thermal comfort index. The WBGT index was developed in the 1950s by the US military to help prevent heat-related illnesses in training camps (Budd, 2008). It has been widely utilized to establish heat safety guidelines and mitigate heat-related illnesses (ISO, 2017), making it suitable for evaluating thermal comfort during heat wave events. WBGT is calculated using the following formula (Yaglou and Minaed, 1957):

$$WBGT = 0.7T_w + 0.2T_g + 0.1T_d \tag{4}$$

where $T_w$ is wet-bulb temperature (°C), $T_g$ is globe temperature (°C), and $T_d$ is dry-bulb temperature (°C) or air temperature. $T_g$ is estimated following Tonouchi et al. (2006) as:

$$T_g - T_d = 0.017S - 0.208U \tag{5}$$

where $S$ is downward solar radiation (in $\mathrm{W/m^2}$) and $U$ is wind speed ($\mathrm{m/s^2}$) that can be estimated using the method presented by Stull (2011):

$$\begin{aligned} T_w =& T_d \tan^{-1}\left[0.151977(\mathrm{RH} + 8.313659)^{1/2}\right] \\ &+ \tan^{-1}(T_d + \mathrm{RH\%}) - \tan^{-1}(\mathrm{RH} - 1.676331) \\ &+ 0.00391838(\mathrm{RH})^{3/2} \tan^{-1}(0.023101\mathrm{RH}) - 4.686035 \end{aligned} \tag{6}$$

where RH denotes relative humidity (in %).

Higher WBGT suggests individuals should engage in less intense activity and take more breaks. WBGT values exceeding 28°C warrant caution as continuous competitive events may require cancelation or rescheduling until heat stress abates. We specifically focus on the threshold of 32°C as the extreme condition (ISO, 2017), a value recognized as the limit beyond which outdoor physical training and intense exercise should be stopped (Armstrong et al., 2007).

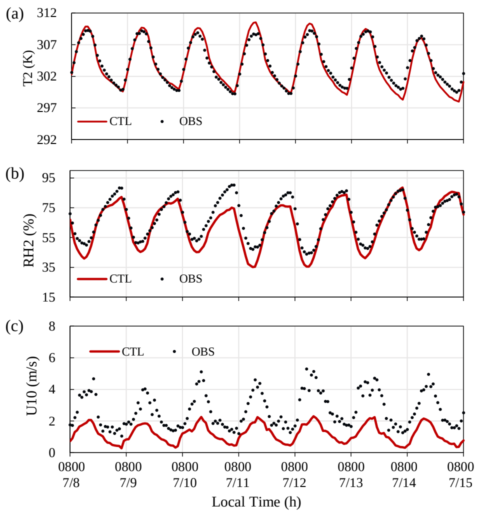


**Fig. 3.** Temporal trends of CTL simulation results compared with observed data (a) 2 m temperature, (b) 2 m relative humidity, (c) 10 m wind speed.

### 2.6. Model evaluation

To assess the ability of the WRF-BEP+BEM to replicate weather conditions in Fuzhou region, Fig.3 presents a comparison of the near-surface diagnostics including T2 (air temperature at 2 m agl), RH2 (relative humidity at 2 m agl), and U10 (wind speed at 10 m agl) averaged from the CTL simulation against observational data collected from seven monitoring sites. The corresponding statistical metrics for each meteorological variable are summarized in Table 2.

Specifically, the T2 values from the CTL simulation align closely with the observed data, exhibiting a mean absolute error of 1.0 °C, a high correlation coefficient of 0.95, and a favorable hit rate of 0.88. RH2 values are generally underestimated compared to observations (Fig.3b), indicating a mean absolute error of 6.9%, a correlation coefficient of 0.95, and a hit rate of 0.76. Notably, the simulation's largest discrepancies with observed values occur during midday and

Journal Pre-proof

nighttime, manifesting as deviations ranging between 10% and 15%.

The U10 of CTL is also significantly underestimated compared with the observations. The simulated data consistently registers 2-3 m/s lower than the observed wind speed (Fig. 3c). Several factors contribute to this disparity. Firstly, the majority of urban sites' Local Climate Zone classifications are designated as "compact" at a 1 km resolution, whereas the observation sites are actually located in open areas at a finer scale of 100 m. Secondly, the complex topography of the Fuzhou region poses challenges that a 1 km grid resolution cannot precisely resolve, consequently introducing errors into the simulations.

In conclusion, the WRF-BEP+BEM model adeptly reproduces the diurnal patterns of temperature, relative humidity, and wind speed within the Fuzhou area throughout the simulation period.

Table 2: Values of statistical indicators for each meteorological variable

| Indicators | T2 (°C) | RH2 (%) | U10 (m/s) |
|---|---|---|---|
| MAE | 1.0 | 6.9 | 1.6 |
| R | 0.95 | 0.95 | 0.67 |
| HR | 0.88 | 0.76 | 0.71 |

## 3. Results and discussion

### 3.1. *Effect of topography and urbanization on thermal comfort*

Figure 4 presents the diurnal cycles of mean near-surface mean meteorological variables and WBGT, averaged over the built-up areas and simulation time, for the CTL scenario. Differences between scenarios reveal the separate and compound impacts of topography and urbanization on thermal comfort. Specifically:

1) Topography effects refer to influences of terrain variation while holding land cover constant. This is quantified by the temperature (as well as other variables) difference between the CTL and NoM scenarios, as well as between NoU and NoMNoU. The no-topography simulations remove the potential for slope flows, altitude-dependent temperature lapse rates, and terrain



Journal Pre-proof

Journal Pre-proof

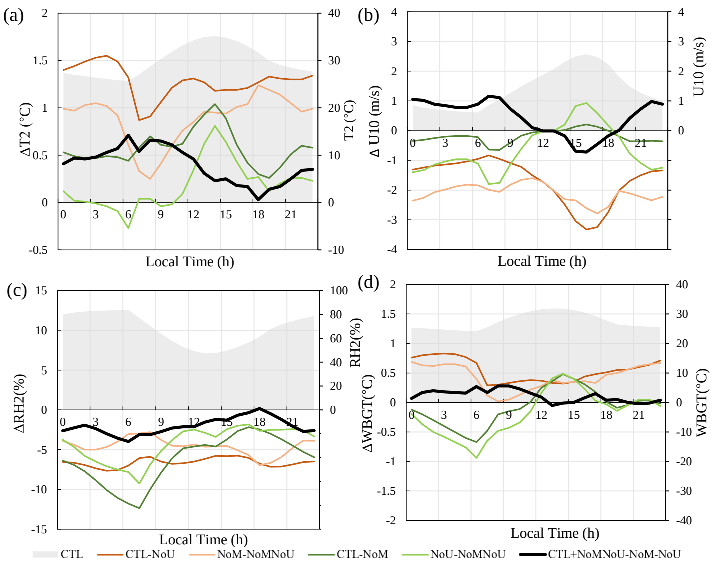


**Fig. 4.** The average diurnal variation at urban grid points for four cases (a) 2 m temperature, (b) 10 m wind speed, (c) 2 m relative humidity, and (d) WBGT

blocking/channeling effects on winds.

2) Urbanization effects encapsulate impacts of realistic LULC change with standard topography. This manifests in the CTL - NoU and NoM - NoMNoU differences. Replacing urban land cover with cropland eliminates anthropogenic heat fluxes as well as contrasts in moisture availability, surface roughness, and radiative properties.

3) The coupled effect accounts for synergies between urbanization and topographic factors that may amplify or dampen one another's thermal comfort consequences. We diagnose this using CTL + NoMNoU - NoM - NoU, where the last two terms remove the individual contributions from points 1) and 2).

In CTL scenario, the mean T2 in the urban area reached a peak of 35.2°C at 1400 LT and a low of 25.7 °C at 0600 LT (Fig. 4a). It is obviously observed that urbanization leads to a warming of

Journal Pre-proof

~ 1 °C in urban areas. Warming is more pronounced during the night, decreases during the latter half of the night, and is at its minimum just before sunrise. The urban structures and impervious surfaces may store solar radiation during daylight hours and slowly release it overnight, leading to slower nocturnal cooling in urban areas. Topographic factors produce significant warming in the afternoon. In general, the urban thermal environment is primarily modulated by surface properties, with terrain exerting a secondary influence. The combined effects of topography and urbanization increase warming during the night and morning, underscoring the compounding effects of these factors on urban thermal dynamics.

In the case of RH2, it decreases after sunrise and begins to rise at 1400LT for the CTL scenario (Fig. 4b). Both urbanization and topography contribute to the reduction of humidity in the urban area. Due to the increase in impervious surfaces and decrease of vegetation in urbanized areas, transpiration diminishes, leading to a reduction in water vapor content. Meanwhile, the warming caused by urbanization also reduces relative humidity. This effect varies less markedly throughout the day. In contrast, the topography's drying impact is more inconsistent day to day, peaking before sunrise.

The diurnal variation of U10 for the CTL scenario follows a similar trend to that of T2, with the maximum onset delayed until 1600 LT (Fig. 4c). The urbanization reduces the wind speeds by 1-3 m/s. The presence of tall buildings and structures in urban regions increases surface roughness and generates greater friction against the flow, effectively slowing down the wind speeds throughout the day. The amplification of the slow-down effect in the afternoon may result from the convergence of flow due to urban heat island circulations. The removal of the topography effect introduces a small wind speed peak at 0800 LT in urban areas, which may attribute to a faster transition from the stable nocturnal boundary layer to a more turbulent daytime state.

According to the WBGT formulation (i.e. eq. 4), higher temperatures and humidity alongside lower wind speeds increase WBGT values. Urbanization increases temperatures and reduces wind speeds, thus raising WBGT consistently despite the drying effects (Fig. 4d). This worsens thermal comfort continuously. Topography primarily exacerbates thermal comfort midday



Journal Pre-proof

Journal Pre-proof

by increasing WBGT. However, during late night and early morning, topography conversely improves comfort. This results mainly from topography's attenuating influence on relative humidity at these times.

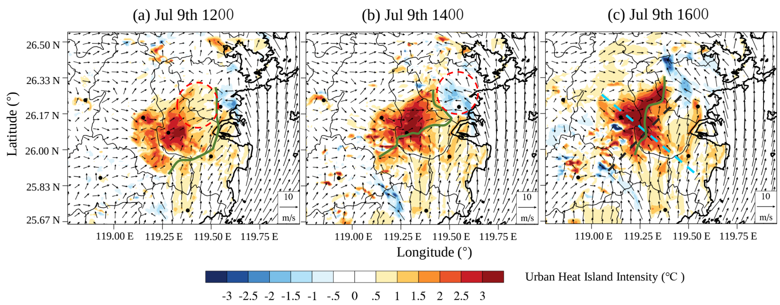


**Fig. 5.** Spatial distribution of the urban heat island intensity (UHII, shaded colors) and the 10 m wind field (vectors) in the CTL scenario on July 9th at (a) 1200 LT, (b) 1400 LT, and (c) 1600 LT, the green solid line represents the sea breeze front of CTL.

Since the highest WBGT and poorest thermal comfort occur during noontime, we further analyze the impacts of topography and urbanization on the near-surface meteorological conditions during this period. For convenience, July 9th is selected as the typical day for investigation based on two reasons: 1) Comparisons of urban heat island intensity (UHII) and near-surface wind fields shows largely similar weather from July 8-13, making the 9th reasonably representative (Fig. S1 - S7). 2) The CTL simulation on July 9th agrees well with observations (Fig. 3), giving higher confidence in result accuracy.

Figure 5 illustrates the spatial distribution of UHII and the 10 m wind fields at three different times for the CTL scenario. The UHII is calculated as the temperature difference between the CTL and NoU scenarios for each model grid cell. At 1200 LT, the sea breeze has not yet reached the CUA. Consequently, the spatial distribution of the urban heat island is relatively uniform across the city. Influenced by the west-to-east land breeze, an "urban wake effect" is evident in the eastern part of Fuzhou city (ref circle in 5a). By 1400 LT, the sea breeze has advanced towards the city center, converging with the land breeze at the sea breeze front. Notably, the

Journal Pre-proof

UHII peaks near this convergence, owing to slowed winds within the obstruction zone where the two breezes meet. This heat accumulation elevates the UHII, which is also observed in previous studies (Ribeiro et al., 2018; Wang et al., 2017). However, a "cool island" phenomenon appears in Lianjiang town as the sea breeze front has passed over (red circle in Fig. 5b). By 1600 LT, the sea breeze front continues inland but progresses shorter distances in the CUA. Due to the continual absorption of solar radiation by the urban surface, the surface temperature continues to rise, leading to a greater urban heat island intensity in the CUA.

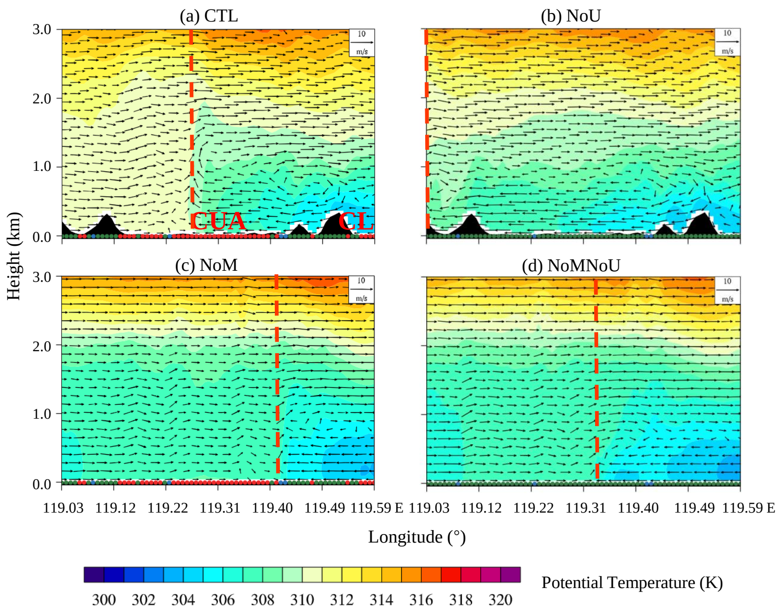


**Fig. 6.** Vertical cross-section of wind (vectors, m $s^{-1}$) and potential temperature (K) (shaded colors) along the blue dashed line in Fig.5 (c) at 1600 LT on July 9th for (a) CTL, (b) NoU, (c) NoM, and (d) NoMNoU scenarios. The vertical wind component is multiplied by a factor of 4. The dots on the $x$ -axis indicate the LULC of each grid, red represents the urban type, green represents the natural type, and blue for the river or ocean type. The red vertical dashed lines represent the locations of the sea breeze front.

Journal Pre-proof

Figure 6 shows the vertical cross-section along the blue line in Fig. 5 (c), and the shaded colors correspond to the potential temperature. In the CTL scenario, the sea breeze and land breeze intersect over the CUA, producing a significant updraft. In contrast, the sea breeze intrudes farther inland without urbanization (NoU). Similarly, a steeper onshore flow front appears over the CUA in the NoM scenario compared to the NoMNoU scenario. This demonstrates that cities hinder the sea breeze penetration regardless of topography, likely due to the UHI circulation and rougher surface in the urban area. Moreover, the inland penetration depth of the sea breeze for both CUA and NoU scenarios surpasses that of scenarios lacking terrain (NoM, NoMNoU). This results from topography channeling the sea breeze inland like side walls. This channeling effect potentially explains the higher afternoon wind speeds in urban areas with terrain variation (Fig. 4b).

Figure 7 shows the vertical cross-section of wind and temperature across the valley at 1500 LT and 1600 LT. Mountains that surround the CUA in the basin restrict airflow, which in turn reduces ventilation and heat dissipation in the afternoon. Additionally, the mountainous terrain triggers a valley wind circulation featuring downdrafts that adiabatically warm the CUA surface, further increasing near-surface temperatures. This explains why deeper intrusion of the cooler sea breeze cannot counteract the warming introduced by the topography (Fig.4 a). Without urbanization (NoU scenario), the valley wind circulation produces clear upslope anabatic winds and downdrafts at 1500 LT and 1600 LT. However, with urbanization, the urban heat island circulation dominates and suppresses the valley wind system. This also induces an earlier transition from upslope wind to downslope wind on the west side of the CUA at 1600 LT (Fig.7 c).

### *3.2. Interplay of the urbanization properties of the CUA and satellite towns*

As noted in Sect. 3.1, a "cool island" phenomenon occurs in the Lianjiang urban area in the afternoons (Fig. 5). Correspondingly, model simulations show a sea breeze invasion in Lianjiang at 1400 LT for the CTL scenario (Fig. 8a), whereas no such sea breeze is found for the NoU scenario at the same moment (Fig. 8b). Vertical cross sections of wind velocity along the red dashed lines (Fig. 8e,f) further reveal a fully developed onshore breeze in CTL but a much weaker



Journal Pre-proof

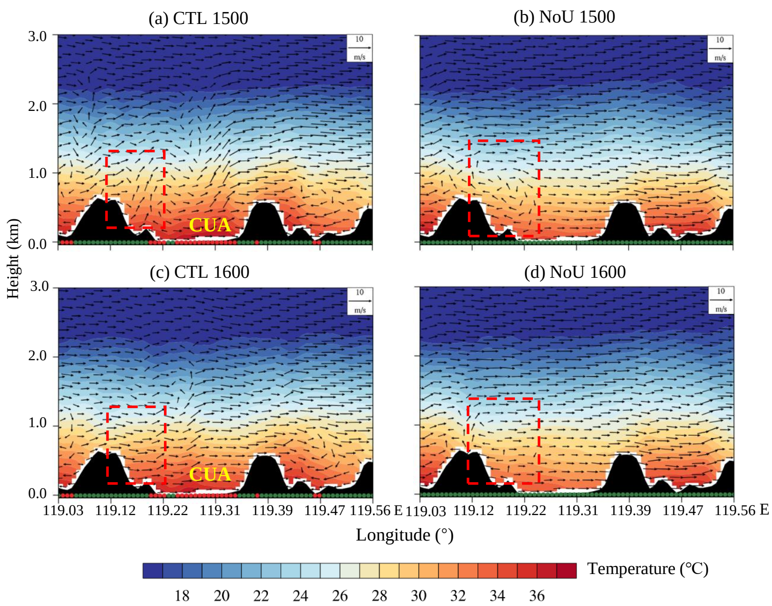


**Fig. 7.** The vertical cross-section of wind and temperature across tne main valley along the black dashed line of Fig.5c at 1500 LT and 1600 LT on July 9th for (a,c) CTL and (b,d) NoU simulations. Vertical wind component is multiplied by a factor of 4.

flow in NoU within the red box. This implies the inland-penetrating sea breeze, facilitated by urbanization, lowers Lianjiang's afternoon temperature and improves its thermal comfort.

An interesting question arises - which part of Fuzhou enables the Lianjiang "cool island" most, the local Lianjiang town or the CUA? The OnlyLJ and OnlyCUA scenarios provide insight. In Fig. 8, the OnlyCUA wind field closely resembles CTL in Lianjiang area, while OnlyLJ resembles NoU. This indicates the increased sea breeze penetration in Lianjiang is not from local urbanization but rather from the CUA. By amplifying the land-sea thermal gradient, urbanization can accelerate sea breezes. However, scale matters: the much larger CUA creates a low-pressure



Journal Pre-proof

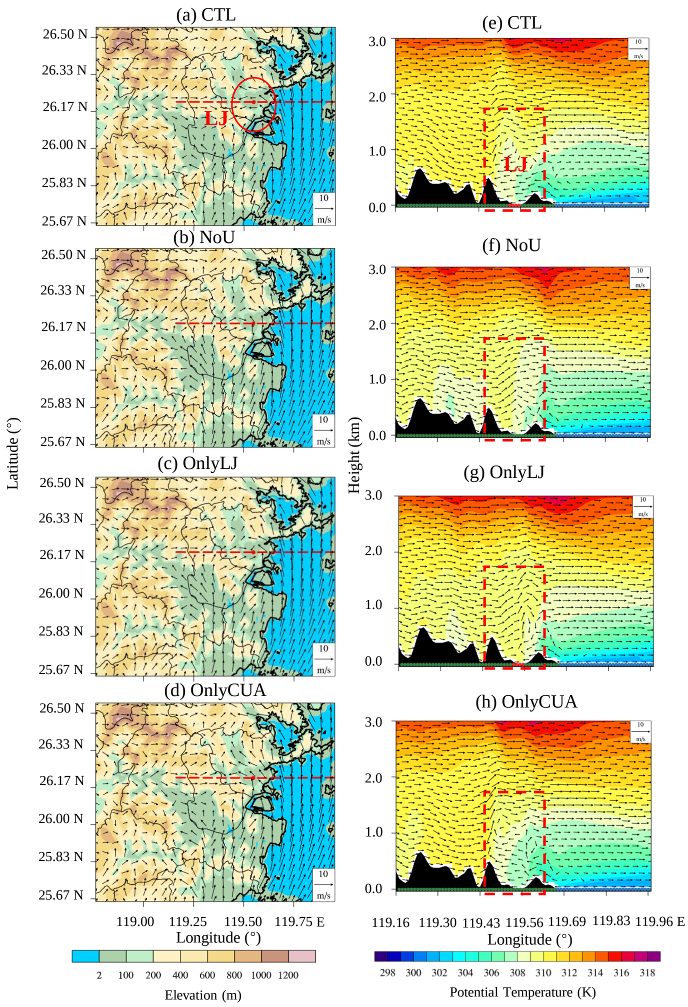


**Fig. 8.** The spatial distribution of 10 m wind and elevation at July 9th, 1400 LT for (a) CTL, (b) NoU, (c) OnlyLJ, (d) OnlyCUA. (e)~(h) are the vertical cross sections of wind along the red dashed lines. Shaded colors in the right panel indicate the potential temperature. The vertical wind component is multiplied by a factor of 4.

Journal Pre-proof

core that propels the cool sea breeze into relatively smaller Lianjiang. The interaction between large urban centres and their smaller suburban counterparts underscores the importance of a holistic approach when examining urban heat islands or thermal comfort in urbanised areas.

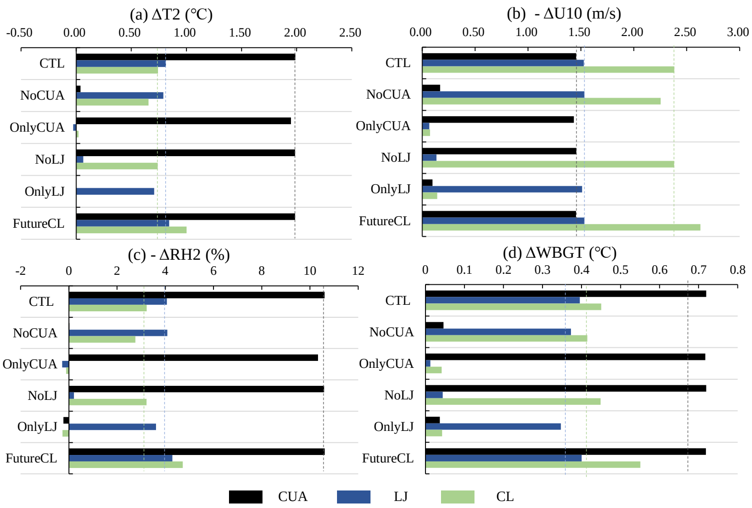


**Fig. 9.** Differences (minus the NoU scenario) of spatiotemporal average (a) T2, (b) U10, (c) RH2, and (d) WBGT over urban areas.

Figure 9 shows the differences in spatiotemporal average meteorological variables and WBGT between the NoU scenario and other scenarios. In the CTL scenario, the warming effect of urbanization is significantly greater in the CUA than in the other satellite towns, due to the concentration of heat release in the dense urban core. However, CUA does not exhibit more pronounced wind speed reductions compared to satellite towns. This complexity arises from that urbanization's impact on wind speed involves more than just localized resistance effects, also modifying mesoscale circulations.

Isolating CUA urbanization (OnlyCUA) reveals that it increases local mean temperatures almost 2°C and WBGT 0.7°C, but with negligible impact on Lianjiang and Changle. Similarly, urbanization in the Lianjiang individually (i.e. OnlyLJ) generates 0.7 °C of local warming with



Journal Pre-proof

Journal Pre-proof

limited impact in most non-urban areas. De-urbanization scenarios (NoCUA and NoLJ) further show urbanization effects are confined locally. Especially, the FutureCL scenario shows that the construction of Binhai New Town can result in an increase of mean WBGT by 0.1°C in CL area. But it has minimal impact on CUA and other satellite towns.

Our simulations suggest a weak interplay in the near-surface thermal environment between the CUA and surrounding satellite towns in the Fuzhou region, which contradicts stronger interactions noted in some megacities like Shanghai-Kunshan (Kang et al., 2014) and Washington-Baltimore (Zhang et al., 2011). The discrepancy implies that, rather than geographic distance, the scale and density of urban development drive the strenth of heat island interactions across cities. This may also be due to the more pronounced effect of local impervious surfaces over aerodynamics on near-surface air UHI (Li et al., 2019). While the localized urban warming provides opportunities to mitigate the deterioration of thermal comfort in CUA, projected urban growth could enhance interactions. This highlights the need to consider differential development and sizes of CUA and satellite towns in regional planning. Continued urban expansion may require coordinated strategies across sub-regions within an urban agglomeration to sustain thermal comfort.

### *3.3. Extreme heat stress*

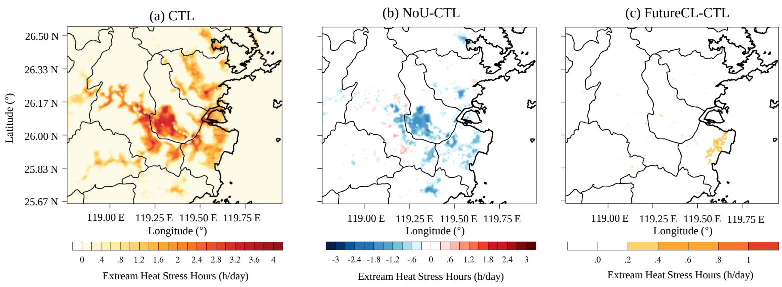


**Fig. 10.** The average number of hours per day during which the WBGT exceeds 32°$C$ for (a) CTL, (c) CTL-NoU scenarios, (b) FutureCL-CTL.

Prior work shows WBGT has a stronger correlation with risks of all-cause mortality, respi-

Journal Pre-proof

ratory hospitalizations, and heat-illness hospitalizations, compared with heat index (HI) and air temperature as indicators of a heat wave (Heo et al., 2019). Analysis of the spatial distribution of hours when WBGT exceeds 32°C, referred to as extreme heat stress hours, reveals the extent of extreme unfavorable thermal conditions experienced by Fuzhou residents (Fig.10). Most lower elevations, except some coastal regions, suffer at least one extreme heat stress hour per day (Fig.1, Fig.10a). Notably, these low-altitude areas overlap significantly with urban regions (Fig.2a). Parts of the central urban area (CUA) endure over 3.5 extreme hours daily. At these levels, outdoor exposure should be reduced even for fit, low-risk individuals to mitigate the high risk of heat illnesses (e.g. exertional heatstroke, heat exhaustion, and exercise-associated muscle cramping) (Armstrong et al., 2007). For children and other vulnerable cohorts, the critical WBGT for canceling exercise needs to be adjusted downward to 29 ~ 30 °C. Prolonged extreme heat also threatens work capacity. For moderate work intensity (300 W), the hourly work capacity of an average worker reduces by 35 % when WBGT exceeds 32°C, based on epidemiological studies conducted by Kjellstrom et al. (2018). With climate change, the summer heat exposure may pose a non-negligible threat to Fuzhou's economic productivity (Casanueva et al., 2020).

Comparing the CTL and NoU scenarios (Fig.10b) shows that the urbanization process contributes to 1 to 2 hours per day of extra extreme heat stress. Figure 10 (c) illustrates the increased exposure to extreme heat stress following the development of Binhai New Town. Building this new town increases localized extreme heat hours by approximately 0.5 hours, implying exacerbated heat stress for residents and workers. Fortunately, the central urban area and other satellite towns do not exhibit extended extreme hours resulting from Changle's development. This suggests that the development of satellite cities or sub-central urban areas, rather than further expansion of the central city, may be a more suitable strategy to accommodate population growth without compromising the thermal environment of existing urban residences.

These results highlight the need for coordinated urban planning and heat mitigation strategies across Fuzhou's metropolitan area. While further urban expansion in the Changle area (Binhai New Town) appears locally contained, urban heat islands remain a pervasive threat. Green space, cool roofs, and reflective materials, which have proven effective in reducing heat exposure



Journal Pre-proof

Journal Pre-proof

(Tan et al., 2023; Yao et al., 2020), may be introduced to alleviate overheating risks in Fuzhou. Meanwhile, other adaptive behaviors like early health warning systems, public education, and preparedness of healthcare facilities are also essential to reduce the adverse effects of high heat stress on health (Kiarsi et al., 2023). As climate change exacerbates heat waves, coordinated efforts across all levels of government and society are essential to develop Fuzhou into a livable and thermal-comfortable city.

### *3.4. Limitations of the modeling approach*

Despite the utility of WRF in aiding investigations into thermal comfort changes under hypothetical scenarios, it must be acknowledged that our methodology, due to its modelling nature, has inherent limitations.

Firstly, we employed WRF model to achieve an optimal balance between computational efficiency and physical detail for the intended simulation domain, timescale, and scientific questions explored. Nonetheless, the 1-km resolution remains insufficient to fully resolve microscale features within the urban canopy. The dependence on parametrizations for turbulence, radiation, and other subgrid-scale processes represents another source of uncertainty. Subsequent studies might utilise more advanced urban canopy models, such as WRF-SUEWS (Sun et al., 2024), at finer resolutions when computational resources permit.

Secondly, validation of the control simulation reveals systematic biases in near-surface temperatures up to 1°C as well as underestimations in RH and wind speeds. Efforts to refine model physics and LCZ classifications at finer resolutions would likely improve the representation of the complex urban environment. Ensembles incorporating parametric uncertainty estimates constitute another avenue for constraining simulations.

Finally, the experiment design only considers a single heatwave period. While useful for characterizing thermal comfort changes between scenarios, the results may not be generalizable across different synoptic conditions. Additionally, the background climate change would likely exacerbate heat stress over longer periods, while urban renewal and development projects unaccounted for here may alter local land covers and thermal dynamics.



Journal Pre-proof

Journal Pre-proof

We acknowledge these limitations not to undermine confidence in our modelling methodology or principal findings, but rather to guide prudent interpretation of the results and encourage further research.

## 4. Conclusions

This study utilized the WRF/BEP-BEM model to investigate the impacts of urbanization and topography on thermal comfort, represented by temperature, humidity, wind speed, and WBGT, in Fuzhou during a heat wave period in 2021. The control run shows the present-day intense urban heat island in the Fuzhou's central urban area (CUA), with rising risks of heat cramps, exhaustion, syncope, and heat stroke for exposed urban residents. Comparisons with scenarios removing urban land use and terrain provided insights into the separate and coupled effects of these two factors.

The key findings are:

(1) The extensive urbanization degrades thermal comfort by raising heat stress city-wide, while complex topography exacerbates midday heat but can alleviate nighttime humidity. The coupled effect of urbanization and topography in deteriorating thermal comfort is greater than the sum of their individual effects.

(2) Urbanization suppresses the penetration of moderate sea breezes regardless of topography guiding their inland advancement. However, the existence of CUA may enhance the sea breeze locally in a satellite town (Lianjiang), inducing a "cool island" effect during afternoons.

(3) Interactions of the mean thermal environment between the CUA and surrounding towns appear minimized, with urbanization impacts confined locally. Furthermore, simulated expansion in Binhai New Town exhibits negligible effects on the thermal comfort in CUA and other satellite towns.

(4) The residents in Fuzhou endured up to 4 hours per day of extreme heat stress during this heat wave event, indicating a substantial threat to public health and labor productivity.



Journal Pre-proof

Journal Pre-proof

While the study provides valuable insights, there remain two main limitations that present opportunities for further investigation:

(1) This work analyses a single heat wave event, which may limit the generalisability of the results. Further work including multiple heat wave events would benefit the transferability of proposed measures in this work.

(2) This study omitted factors such as CUA renewal and the expansion of satellite towns – crucial elements to consider when evaluating the effects of urbanization on local thermal comfort. To fully assess future thermal comfort across Fuzhou's metropolitan area, it is essential to incorporate these local dynamics.

This work reveals a persistent urban heat island in Fuzhou owing to its geographical uniqueness. Though future development according to the Fuzhou2035 Plan may not impact CUA, it could degrade Binhai New Town's thermal comfort. Thus, sustainable development requires implementing holistic mitigation strategies in both developed and developing districts of Fuzhou.



Journal Pre-proof

Journal Pre-proof

**List of Abbreviations**

| | |
|---|---|
| BEM | Building Energy Model |
| BEP | Building Effects Parameterization |
| CL | Changle |
| CTL | control |
| CUA | central urban area |
| FutureCL | Future Changle |
| Fuzhou2035 | Fuzhou Master Plan 2021-2035 |
| FZ | Fuzhou |
| HR | hit rate |
| LCZ | local climate zone |
| LJ | Lianjiang |
| LULC | Land use and land cover |
| MAE | mean absolute error |
| NoCUA | No central urban area |
| NoLJ | No Lianjiang |
| NoM | No Moutains |
| NoMNoU | No Moutains and No Urbanization |
| NoU | No Urbanization |
| OnlyCUA | Only central urban area |
| OnlyLJ | Only Lianjiang |
| R | correlation corfficient |
| RH2 | relative humidity at 2 m agl |
| T2 | air temperature at 2 m agl |
| U10 | wind speed at 10 m agl |
| UHI | urban heat island |
| UHII | urban heat island intensity |
| WBGT | Wet Bulb Globe Temperature |
| WRF | Weather Research and Forecasting model |

**Acknowledgments**

This work is supported by the Young Scientist Program of Fujian Province Natural Science Foundation (Grant No. 2021J05125), and Key Laboratory of Urban Meteorology, China Meteorological Administration (LUM-2023-14). TS is supported by UKRI NERC Independent Re-



Journal Pre-proof

search Fellowship (NE/P018637/2). YC is supported by the Natural Science Foundation of China (Grants No. 42205075) and the youth innovation team of China Meteorological Administration (No. CMA2023QN14).

### Statement

During the preparation of this work, the authors used Claude to improve the language. After using this tool/service, the authors reviewed and edited the content as needed and take full responsibility for the content of the publication.

### References

Armstrong, L.E., Casa, D.J., Millard-Stafford, M., Moran, D.S., Pyne, S.W., Roberts, W.O., 2007. Exertional heat illness during training and competition. Medicine & Science in Sports & Exercise 39, 556–572. doi:10.1249/MSS.0b013e31802fa199.

Brousse, O., Martilli, A., Foley, M., Mills, G., Bechtel, B., 2016. Wudapt, an efficient land use producing data tool for mesoscale models? integration of urban lcz in wrf over madrid. Urban Climate 17, 116–134. URL: https://www.sciencedirect.com/science/article/pii/S2212095516300219, doi:https://doi.org/10.1016/j.uclim.2016.04.001.

Budd, G.M., 2008. Wet-bulb globe temperature (wbgt)—its history and its limitations. Journal of Science and Medicine in Sport 11, 20–32. doi:10.1016/j.jsams.2007.07.003.

Cai, Y., Chen, Y., Tong, C., 2019. Spatiotemporal evolution of urban green space and its impact on the urban thermal environment based on remote sensing data: A case study of fuzhou city, china. Urban Forestry & Urban Greening 41, 333–343. doi:10.1016/j.ufug.2019.04.012.

Casanueva, A., Kotlarski, S., Fischer, A.M., Flouris, A.D., Kjellstrom, T., Lemke, B., Nybo, L., Schwierz, C., Liniger, M.A., 2020. Escalating environmental summer heat exposure—a future threat for the european workforce. Regional Environmental Change 20, 40. URL: https://doi.org/10.1007/s10113-020-01625-6, doi:10.1007/s10113-020-01625-6.

China Meteorological Administration, 2012. National climate center expert: More and more "furnace" cities URL: http://www.cma.gov.cn/2011xwzx/2011xqhbh/2011xdtxx/201208/t20120816_182112.html.

Choudhury, D., Das, A., Das, M., 2021. Investigating thermal behavior pattern (tbp) of local climatic zones (lczs): A study on industrial cities of asansol-durgapur development area (adda), eastern india. Urban Climate 35. doi:10.1016/j.uclim.2020.100727.

Demuzere, M., Argüeso, D., Zonato, A., Kittner, J., 2022. W2w: A python package that injects wudapt's local climate zone information in wrf. Journal of Open Source Software 7. doi:10.21105/joss.04432.



Journal Pre-proof

Journal Pre-proof

Demuzere, M., Kittner, J., Bechtel, B., 2021. Lcz generator: A web application to create local climate zone maps. Frontiers in Environmental Science 9. doi:10.3389/fenvs.2021.637455.

Dudhia, J., 1989. Numerical study of convection observed during the winter monsoon experiment using a mesoscale two-dimensional model. Journal of Atmospheric Sciences 46, 3077–3107.

Dutta, P., Sathish, L., Mavankar, D., Ganguly, P.S., Saunik, S., 2020. Extreme heat kills even in very hot cities: Evidence from nagpur, india. Int J Occup Environ Med 11, 188–195. URL: https://www.ncbi.nlm.nih.gov/pubmed/33098403, doi:10.34172/ijoem.2020.1991.

Epstein, Y., Moran, D.S., 2006. Thermal comfort and the heat stress indices. Industrial health 44, 388–398.

Fernando, H.J.S., 2010. Fluid dynamics of urban atmospheres in complex terrain. Annual Review of Fluid Mechanics 42, 365–389. doi:10.1146/annurev-fluid-121108-145459.

Fuzhou Municipal Statistics Bureau, 2021. Bulletin of the 7th national census of fuzhou URL: http://tjj.fuzhou.gov.cn/zz/zwgk/tjzl/ndbg/202105/t20210524_4104989.htm.

Ganbat, G., Seo, J.M., Han, J.Y., Baik, J.J., 2014. A theoretical study of the interactions of urban breeze circulation with mountain slope winds. Theoretical and Applied Climatology 121, 545–555. doi:10.1007/s00704-014-1252-6.

Garuma, G.F., 2018. Review of urban surface parameterizations for numerical climate models. Urban Climate 24, 830–851.

Grell, G.A., Dévényi, D., 2002. A generalized approach to parameterizing convection combining ensemble and data assimilation techniques. Geophysical Research Letters 29, 38–1–38–4. doi:10.1029/2002gl015311.

Heo, S., Bell, M.L., Lee, J.T., 2019. Comparison of health risks by heat wave definition: Applicability of wet-bulb globe temperature for heat wave criteria. Environmental Research 168, 158–170. doi:10.1016/j.envres.2018.09.032.

Hong, S.Y., Noh, Y., Dudhia, J., 2006. A new vertical diffusion package with an explicit treatment of entrainment processes. Monthly weather review 134, 2318–2341.

Howard, L., 1833. The climate of London: deduced from meteorological observations made in the metropolis and at various places around it. volume 3. Harvey and Darton, J. and A. Arch, Longman, Hatchard, S. Highley and R. Hunter.

Huang, Q., Huang, J., Yang, X., Fang, C., Liang, Y., 2019. Quantifying the seasonal contribution of coupling urban land use types on urban heat island using land contribution index: A case study in wuhan, china. Sustainable Cities and Society 44, 666–675.

Ibrahim, S.H., Ibrahim, N.I.A., Wahid, J., Goh, N.A., Koesmeri, D.R.A., Nawi, M.N.M., 2018. The impact of road pavement on urban heat island (uhi) phenomenon. Civil Engineering 9.

ISO, ., 2017. Ergonomics of the thermal environment—assessment of heat stress using the wbgt (wet bulb globe temperature) index. Geneva: International Organization for Standardization .

Kang, H.Q., Zhu, B., Zhu, T., Sun, J.L., Ou, J.J., 2014. Impact of megacity shanghai on the urban heat-island effects over the downstream city kunshan. Boundary-Layer Meteorology 152, 411–426. doi:10.1007/s10546-014-9927-1.

Kiarsi, M., Amiresmaili, M., Mahmoodi, M.R., Farahmandnia, H., Nakhaee, N., Zareiyan, A., Aghababaeian, H., 2023.



Journal Pre-proof

Journal Pre-proof

Heat waves and adaptation: A global systematic review. J Therm Biol 116, 103588. URL: https://www.ncbi.nlm.nih.gov/pubmed/37499408, doi:10.1016/j.jtherbio.2023.10358810.1016/j.jtherbio.2023.103588.Epub2023Jul16.

Kjellstrom, T., Freyberg, C., Lemke, B., Otto, M., Briggs, D., 2018. Estimating population heat exposure and impacts on working people in conjunction with climate change. International Journal of Biometeorology 62, 291–306. URL: https://doi.org/10.1007/s00484-017-1407-0, doi:10.1007/s00484-017-1407-0.

Li, D., Liao, W., Rigden, A.J., Liu, X., Wang, D., Malyshev, S., Shevliakova, E., 2019. Urban heat island: Aerodynamics or imperviousness? Science Advances 5, eaau4299. URL: https://www.science.org/doi/abs/10.1126/sciadv.aau4299, doi:doi:10.1126/sciadv.aau4299.

Li, Y., Schubert, S., Kropp, J.P., Rybski, D., 2020. On the influence of density and morphology on the urban heat island intensity. Nature communications 11, 1–9.

Liu, S., Liu, Z., Li, J., Wang, Y., Ma, Y., Sheng, L., Liu, H., Liang, F., Xin, G., Wang, J., 2009. Numerical simulation for the coupling effect of local atmospheric circulations over the area of beijing, tianjin and hebei province. Science in China Series D: Earth Sciences 52, 382–392. doi:10.1007/s11430-009-0030-2.

Lüthi, S., Fairless, C., Fischer, E.M., Scovronick, N., Ben, A., Coelho, M.D.S.Z.S., Guo, Y.L., Guo, Y., Honda, Y., Huber, V., Kyselý, J., Lavigne, E., Royé, D., Ryti, N., Silva, S., Urban, A., Gasparrini, A., Bresch, D.N., Vicedo-Cabrera, A.M., 2023. Rapid increase in the risk of heat-related mortality. Nature Communications 14. doi:10.1038/s41467-023-40599-x.

Martilli, A., Clappier, A., Rotach, M.W., 2002. An urban surface exchange parameterisation for mesoscale models. Boundary-layer meteorology 104, 261–304. doi:10.1023/A:1016099921195.

Mehrotra, S., Bardhan, R., Ramamritham, K., 2019. Outdoor thermal performance of heterogeneous urban environment: An indicator-based approach for climate-sensitive planning. Science of the Total Environment 669, 872–886.

Miao, Y., Liu, S., Zheng, Y., Wang, S., Chen, B., 2015. Numerical study of the effects of topography and urbanization on the local atmospheric circulations over the beijing-tianjin-hebei, china. Advances in Meteorology 2015, 1–16. doi:10.1155/2015/397070.

Ministry of Housing and Urban-Rural Development, PRC, 2011. Gb 50137-2011: Code for classification of urban land use and planning standards of development land (in chinese). General Administration of Quality Supervision, Inspection and Quarantine of the People's Republic of China .

Mlawer, E.J., Taubman, S.J., Brown, P.D., Iacono, M.J., Clough, S.A., 1997. Radiative transfer for inhomogeneous atmospheres: Rrtm, a validated correlated-k model for the longwave. Journal of Geophysical Research: Atmospheres 102, 16663–16682. doi:10.1029/97jd00237.

Molnár, G., Gyöngyösi, A.Z., Gál, T., 2019. Integration of an lcz-based classification into wrf to assess the intra-urban temperature pattern under a heatwave period in szeged, hungary. Theoretical and Applied Climatology 138, 1139–1158. URL: https://link.springer.com/content/pdf/10.1007/s00704-019-02881-1.pdf, doi:10.1007/s00704-019-02881-1.



Journal Pre-proof

Journal Pre-proof

National Centers for Environmental Prediction, National Weather Service, NOAA, U.S. Department of Commerce, 2000. Ncep fnl operational model global tropospheric analyses, continuing from july 1999. URL: https://doi.org/10.5065/D6M043C6.

Niu, G.Y., Yang, Z.L., Mitchell, K.E., Chen, F., Ek, M.B., Barlage, M., Kumar, A., Manning, K., Niyogi, D., Rosero, E., Tewari, M., Xia, Y., 2011. The community noah land surface model with multiparameterization options (noah-mp): 1. model description and evaluation with local-scale measurements. Journal of Geophysical Research 116. doi:10.1029/2010jd015139.

Oke, T.R., 1995. The heat island of the urban boundary layer: characteristics, causes and effects. Springer. pp. 81–107.

Oke, T.R., Stewart, I.D., 2012. Local climate zones for urban temperature studies. Bulletin of the American Meteorological Society 93, 1879–1900. doi:10.1175/bams-d-11-00019.1.

Pellegatti Franco, D.M., Andrade, M.d.F., Ynoue, R.Y., Ching, J., 2019. Effect of local climate zone (lcz) classification on ozone chemical transport model simulations in sao paulo, brazil. Urban Climate 27, 293–313. doi:10.1016/j.uclim.2018.12.007.

Ribeiro, F.N.D., Oliveira, A.P.d., Soares, J., Miranda, R.M.d., Barlage, M., Chen, F., 2018. Effect of sea breeze propagation on the urban boundary layer of the metropolitan region of sao paulo, brazil. Atmospheric Research 214, 174–188. doi:10.1016/j.atmosres.2018.07.015.

Ryu, Y.H., Baik, J.J., 2013. Daytime local circulations and their interactions in the seoul metropolitan area. Journal of Applied Meteorology and Climatology 52, 784–801. doi:10.1175/jamc-d-12-0157.1.

Salamanca, F., Krpo, A., Martilli, A., Clappier, A., 2010. A new building energy model coupled with an urban canopy parameterization for urban climate simulations—part i. formulation, verification, and sensitivity analysis of the model. Theoretical and applied climatology 99, 331–344.

Sanchez, B., Roth, M., Simón-Moral, A., Martilli, A., Velasco, E., 2021. Assessment of a meteorological mesoscale model's capability to simulate intra-urban thermal variability in a tropical city. Urban Climate 40. doi:10.1016/j.uclim.2021.101006.

Shen, C., Hou, H., Zheng, Y., Murayama, Y., Wang, R., Hu, T., 2022. Prediction of the future urban heat island intensity and distribution based on landscape composition and configuration: A case study in hangzhou. Sustainable Cities and Society 83. doi:10.1016/j.scs.2022.103992.

Skamarock, W.C., Klemp, J.B., Dudhia, J., Gill, D.O., Barker, D.M., Wang, W., Powers, J.G., 2021. A description of the advanced research wrf model version 4.3(july) doi:10.5065/1dfh-6p97.

Stull, R., 2011. Wet-bulb temperature from relative humidity and air temperature. Journal of applied meteorology and climatology 50, 2267–2269.

Sun, T., Omidvar, H., Li, Z., Zhang, N., Huang, W., Kotthaus, S., Ward, H.C., Luo, Z., Grimmond, S., 2024. WRF (v4.0)–SUEWS (v2018c) coupled system: development, evaluation and application. Geoscientific Model Development 17, 91–116. doi:10.5194/gmd-17-91-2024.

Tan, H., Kotamarthi, R., Wang, J., Qian, Y., Chakraborty, T.C., 2023. Impact of different roofing mitigation strategies



Journal Pre-proof

Journal Pre-proof

on near-surface temperature and energy consumption over the chicago metropolitan area during a heatwave event. Science of The Total Environment 860. doi:10.1016/j.scitotenv.2022.160508.

Thompson, G., Rasmussen, R.M., Manning, K., 2004. Explicit forecasts of winter precipitation using an improved bulk microphysics scheme. part i: Description and sensitivity analysis. Monthly Weather Review 132, 519–542.

Tonouchi, M., Murayama, K., Ono, M., 2006. Wbgt forecast for preventing heat strokes in japan, in: Sixth symposium on the urban environment. American Meteorological Society, Section PJ1.

United Nations, 2020. Department of Economic and Social Affairs, Population Division. World Population Prospects 2019: Highlights. Report.

Vinayak, B., Lee, H.S., Gedam, S., Latha, R., 2022. Impacts of future urbanization on urban microclimate and thermal comfort over the mumbai metropolitan region, india. Sustainable Cities and Society 79. doi:10.1016/j.scs.2022.103703.

Wang, W., Wang, X., Ng, E., 2021. The coupled effect of mechanical and thermal conditions on pedestrian-level ventilation in high-rise urban scenarios. Building and Environment 191, 107586.

Wang, Y., Di Sabatino, S., Martilli, A., Li, Y., Wong, M.S., Gutiérrez, E., Chan, P.W., 2017. Impact of land surface heterogeneity on urban heat island circulation and sea-land breeze circulation in hong kong. Journal of Geophysical Research: Atmospheres 122, 4332–4352. doi:10.1002/2017jd026702.

Wang, Y., Li, X., Zhang, C., He, W., 2022. Influence of spatiotemporal changes of impervious surface on the urban thermal environment: A case of huai'an central urban area. Sustainable Cities and Society 79. doi:10.1016/j.scs.2022.103710.

Wu, S., Wang, Y., Chen, C., Cao, Z., Cao, J., Yu, Z., Song, H., 2021. Valley city ventilation under the calm and stable weather conditions: A review. Building and Environment 194. doi:10.1016/j.buildenv.2021.107668.

Xiao, Z., Liang, S., Wang, J., Xiang, Y., Zhao, X., Song, J., 2016. Long-time-series global land surface satellite leaf area index product derived from modis and avhrr surface reflectance. IEEE Transactions on Geoscience and Remote Sensing 54, 5301–5318. doi:10.1109/tgrs.2016.2560522.

Yaglou, C., Minaed, D., 1957. Control of heat casualties at military training centers. Arch. Indust. Health 16, 302–16.

Yang, L., Yu, K., Ai, J., Liu, Y., Lin, L., Lin, L., Liu, J., 2021. The influence of green space patterns on land surface temperature in different seasons: A case study of fuzhou city, china. Remote Sensing 13. doi:10.3390/rs13245114.

Yang, Z.L., Niu, G.Y., Mitchell, K.E., Chen, F., Ek, M.B., Barlage, M., Longuevergne, L., Manning, K., Niyogi, D., Tewari, M., Xia, Y., 2011. The community noah land surface model with multiparameterization options (noah-mp): 2. evaluation over global river basins. Journal of Geophysical Research 116. doi:10.1029/2010jd015140.

Yao, L., Li, T., Xu, M., Xu, Y., 2020. How the landscape features of urban green space impact seasonal land surface temperatures at a city-block-scale: An urban heat island study in beijing, china. Urban Forestry & Urban Greening 52. doi:10.1016/j.ufug.2020.126704.

Yao, X., Zeng, X., Zhu, Z., Lan, Y., Shen, Y., Liu, Q., Yang, F., 2023. Exploring the diurnal variations of the driving factors affecting block-based lst in a "furnace city" using ecostress thermal imaging. Sustainable Cities and Society



Journal Pre-proof

98, 104841. doi:https://doi.org/10.1016/j.scs.2023.104841.

Yao, X., Zhu, Z., Zeng, X., Huang, S., Liu, Q., Yu, K., Zhou, X., Chen, Z., Liu, J., 2022. Linking maximum-impact and cumulative-impact indices to quantify the cooling effect of waterbodies in a subtropical city: A seasonal perspective. Sustainable Cities and Society 82. doi:10.1016/j.scs.2022.103902.

You, M., Lai, R., Lin, J., Zhu, Z., 2021. Quantitative analysis of a spatial distribution and driving factors of the urban heat island effect: A case study of fuzhou central area, china. Int J Environ Res Public Health 18. URL: https://www.ncbi.nlm.nih.gov/pubmed/34948699, doi:10.3390/ijerph182413088.

Zhang, D., Anthes, R.A., 1982. A high-resolution model of the planetary boundary layer—sensitivity tests and comparisons with sesame-79 data. Journal of Applied Meteorology 21, 1594–1609.

Zhang, D.L., Shou, Y.X., Dickerson, R.R., 2009. Upstream urbanization exacerbates urban heat island effects. Geophysical Research Letters 36. doi:10.1029/2009gl041082.

Zhang, D.L., Shou, Y.X., Dickerson, R.R., Chen, F., 2011. Impact of upstream urbanization on the urban heat island effects along the washington–baltimore corridor. Journal of Applied Meteorology and Climatology 50, 2012–2029. doi:10.1175/jamc-d-10-05008.1.

Zhou, X., Yamamoto, M., Yan, S., Ishida, Y., Cai, M., Ji, Q., Makvandi, M., Li, C., 2022. Exploring the impacts of heat release of vehicles on urban heat mitigation in sendai, japan using wrf model integrated with urban lcz. Sustainable Cities and Society 82. doi:10.1016/j.scs.2022.103922.



Journal Pre-proof

Highlights

- We model a heat wave event in Fuzhou, China using WRF to assess human thermal comfort
- Urbanization elevates heat stress citywide while topography exacerbates midday heat.
- Urbanization of the central urban area (CUA) helps the sea breeze penetrate a satellite town.
- Urbanization in CUA and satellite towns weakly affects each other's thermal environments.
- The expansion in Binhai New Town has minimal impact on the thermal comfort in CUA.

Journal Pre-proof

Journal Pre-proof

**Declaration of Interest statement**

We declare that we have no financial and personal relationship with any other people or organizations that could inappropriately influence (bias) our work. There are no potential conflicts of interest include employment, consultancies, stock ownership, honoraria, paid expert testimony, patent applications/registrations, and grants or other funding.

Journal Pre-proof